INTERACTIVE CONTROL ENGINEERING
Principles and Applications

Volume 20 Motion Control, Robotics, and Autonomous Systems

CHAPTER 14

Surgical Robot Simulator for Control Through a Fixed Port onto Moving Tissue

Pages 329–353

Edited by John D. Hedengren

How to cite this chapter. "Surgical Robot Simulator for Control Through a Fixed Port onto Moving Tissue," in *Motion Control, Robotics, and Autonomous Systems*, John D. Hedengren, Ed., vol. 20 of *Interactive Control Engineering: Principles and Applications*. Advanced Process Solutions, LLC, 2026, ch. 14, pp. 329–353.

The page numbers in this file are those of the printed volume.

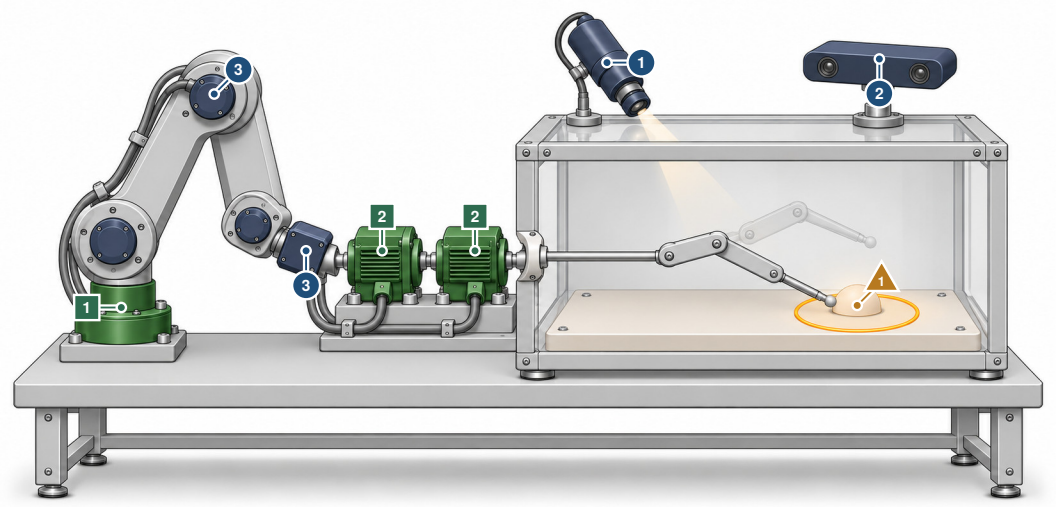
The app for this chapter
https://apmonitor.com/apps/surgical-robot/

The volume online: contents, other chapters and citation records
https://apmonitor.com/apps/books/v20-motion-robotics/#surgical-robot

Copyright © 2026 Advanced Process Solutions, LLC. All rights reserved. Produced by Advanced Process Solutions, LLC.

CHAPTER 14

Surgical Robot Simulator for Control Through a Fixed Port onto Moving Tissue



The controller moves 1 arm drives that pivot the shaft about the port and slide it in 2 drives that pull the wrist's cables

The controller reads 1 endoscope camera, the late picture the surgeon steers by
2 tissue tracker that reports the organ's motion late 3 joint encoders on the arm

What disturbs it 1 the organ's motion with each breath or heartbeat

Notice that the instrument pivots about the fixed port in the box wall, that no sensor reads the force at the tip, and that the target moves while the camera and the tracker see it late. Illustration, not to scale.

IN PLAIN TERMS A Robot Between the Hand and the Patient

The main idea. In keyhole surgery, long tools pass through small cuts in the belly. The tip then moves the opposite way to the hand. A surgical robot undoes that flip, and it can shrink and smooth the hand's motion before it reaches the tip.

The challenge. Each helper has a price. Smoothing out the shake of the hand adds a delay that the surgeon does not expect, and the organs keep moving with every breath, so the robot has to guess where they will be.

Why it matters. Knowing what each layer fixes and what it costs tells a designer which errors a robot can remove and which it cannot.

THREE WAYS TO READ THIS CHAPTER

⊘	**Explore**	12 min	the first page, the two history segments (Section 14.2), the fact on robotic surgery's spread (Section 14.5), the try-it segments of cases 3 and 8 and the fact on the error budget (Sections 14.5 and 14.5.6) and the key points
🕮	**Study**	50 min	the whole chapter with its three pause points and the twelve exercises at its end
⌓	**Practice**	20 min	the first page, the measured cases (Section 14.5), Technology in Practice (Section 14.6), Limitations (Section 14.7) and the open challenges

The control question A surgical robot inverts the fulcrum of the port, scales and filters the hand, holds tissue with a force loop on an estimate and forecasts the patient's breathing. How much of the tip error does each layer remove, and what does each one cost?

Learning objectives

- Compute the lever ratio of a hand-held instrument and the tip speed that a pivot rate limit allows at a given insertion.
- Explain how a tremor filter trades tremor at the tip against a lag that the surgeon's forward model does not expect.
- Predict the relaxation, creep and tear of a standard linear solid under a position hold and under a force loop on a biased estimate.
- Compare ventilator feedforward, an adaptive harmonic predictor and MPC on a breathing organ, and read a factorial error budget.
- Recognize a disturbance that no setting can reject, as on the beating heart.

Prerequisites Sections 1.6.2 (velocity form), 1.4.8 (force loop through a stiffness), 1.4.6 (report age), 1.4.9 (checking a monitor against the truth) and 1.4.10 (error budgets). Section 1.6.3 is needed only for the MPC option, and Chapter 13 is a gentler first force loop.

The app https://apmonitor.com/apps/surgical-robot/

See also Volume 5, Chapter 8 for the delayed force channel this chapter leaves out, and Volume 5, Chapter 13 for late fixes applied at the instant they describe. Volume 7, Chapter 13 for a vibration that repeats every tooth, and Volume 7, Chapter 12 for a feedforward canceler built on an assumed model.

14.1 Introduction

A straight grasper held by its handle passes through a port in the abdominal wall with 120 mm of shaft inside the patient and 240 mm outside. When the hand moves 20 mm to the right, the tip moves 9.90 mm to the left. Pushed 80 mm further in, the same 20 mm of hand motion moves the tip 24.65 mm the other way. The port is a fulcrum, and its lever arms change every time the surgeon changes the depth. A surgical robot removes that reversal by solving, many times a second, for the pivots and the insertion that put the tip where the hand went. It then adds layers of its own: a scale and a filter between the hand and the command, a loop on a force it estimates rather than measures, a rule that keeps the tool out of a region on a map, and a forecast of where a breathing organ will be when the command reaches it. Each of these runs in the simulator of this chapter, and each has a cost that the simulator measures.

The plant corrects four beliefs that a block diagram of a teleoperator leaves in place. The first is that the robot copies the hand. It does not, and near the port the inversion that undoes the fulcrum asks the shaft for more rate than it has, so the tip falls up to 51.5 mm behind its command. The second is that more filtering is safer. A 2 Hz tremor filter cuts the tremor at the tip to 12 µm but adds 120 ms of lag that the surgeon's eye-hand loop does not expect, and three dissection strokes overshoot into an artery that a 6 Hz filter never touches. The third is that a force held below the tissue's tear force is safe. A force loop at 2.5 N on a flap that tears at 3 N lets the flap creep until its stretch tears it at 13.3 s. The fourth is that a faster sensor defeats a fast disturbance. Behind a tracker 40 ms late or 200 ms late, no option holds the tip within 1 mm of a coronary artery on a beating heart, and the best does 1.53 mm.

The problem belongs to a wider class, motion through a kinematic constraint with a human in the loop, acting on a load that relaxes and that moves with a disturbance whose period, or whose phase, is measured. A periodic exogenous signal is the object of repetitive control, which places a model of the period inside the loop [1]. Roll eccentricity in a strip mill, blade passing in a rotating machine, the tooth-passing vibration of the end mill of Volume 7, Chapter 13, a cyclic process with a recipe clock and the beating of a heart share that structure, and the surgical form has been treated with predictive control on the respiratory cycle [2] and on the heartbeat [3]. The fixed remote center is a holonomic

constraint on the shaft, built into the mechanism of the arms that hold laparoscopic instruments [4, 5], and it turns a hand's motion into joint rates that grow without bound as the tip nears the port.

However, the published motion compensation, virtual fixtures, tremor cancellation and autonomous suturing are each demonstrated on their own platform [2, 6–8], and a student cannot change one layer of a surgical robot at a time and see what each costs on the same seed. This chapter apportions how much of a surgical robot's tip error comes from the fulcrum, the console, the tissue and the patient's motion, and which control element removes which, using a browser simulator with eleven procedure excerpts and a challenge. The remote center, the standard linear solid, the three-phase needle force, harmonic prediction by recursive least squares, the forbidden-region fixture and supervised autonomy are all established [5, 7–10], and the chapter uses them as they stand. Its analysis is a two-level factorial error budget, measured on the running engine over five seeds, in which the surgeon's visuomotor delay costs nothing on a still mark and 86 % of the mean-square error on a breathing one, and an adaptive harmonic predictor removes 91 % of that interaction. A forecast taken on the ventilator's phase makes the tracker's latency almost irrelevant from 40 to 200 ms, and without compensation not one of 240 bites on a breathing kidney is kept, whatever else is removed. The model has 28 states, and its controllers read a measurement packet and never the simulator's truth. The surgeon is scripted with an internal forward model, and the recursive least-squares update is written in symmetric form because the textbook form diverged. Every case and the challenge carry a rule that awards credit when it is met (Section 1.6.4).

Section 14.2 traces the domain from stereotaxy to supervised suturing. Section 14.3 gives the instrument, the tissue, the patient's motion, the sensors and the scripted surgeon as simulated, and Section 14.4 gives the controllers as coded: the console, the virtual fixtures, the force loop, motion compensation and the autonomous suturing subtask. Section 14.5 reports the cases as measured, with the error budget in Section 14.5.6. Section 14.6 names the devices of real surgical robots, Section 14.7 states the limitations, Section 14.8 summarizes the results, and the exercises follow in Section 14.9.

14.2 From Stereotaxy to Supervised Suturing

Robots entered the operating room as positioners, and the history segment below follows the first of them and the fulcrum effect that laparoscopy put on the hand.

> ⧖ HISTORY **From Positioner to Fulcrum, 1988 to 1998**
>
> In 1988 a robot for stereotactic brain surgery guided by computed tomography was reported, and the report was about improving the robot's absolute positioning accuracy [11]. Laparoscopic surgery put a different burden on the hand, because the abdominal wall acts as a fulcrum on every instrument that passes through it. An ergonomic study of 1998 had novices make defined incisions under laparoscopic laboratory conditions. Those who worked with the image's vertical axis inverted made more incisions, and more correct ones, than those with a normal image, and the difference persisted over 50 trials. The study concluded that the fulcrum effect has a major detrimental influence on the acquisition of endoscopic skill [12].

The first robots inside the abdomen held the camera or an instrument for the surgeon. A telerobotic assistant for laparoscopy, reported in 1995, was built around a remote-center-of-motion mechanism so that the instrument pivoted about the port by construction [4]. By 2003 a review of computer-integrated surgery could describe a family of such systems, from robots that execute a plan made on images to assistants that work beside the surgeon, many of them on a remote center [5]. The console-based platforms in clinical use gave the surgeon no sense of the force at the tip, so force control stayed visual [13]. In 2001 a cholecystectomy was performed on a patient in Strasbourg by surgeons in New York over a dedicated network, a demonstration that the console and the patient could be an ocean apart [14]. The delay and passivity questions that long distance raises are the subject of Volume 5, Chapter 8 and are left out here.

The control literature turned next to what the hand cannot do. Adaptive cancellation of physiological tremor, a band near 10 Hz that a human cannot suppress, was demonstrated for microsurgery in 1998 [6]. Breathing and the heartbeat move the organs under the instruments by millimeters to centimeters, and predictive control with a repetitive model of the respiratory cycle was shown to cancel organ motion on a robot holding an instrument in a live animal [2]. The heart was harder, because its motion is faster, has many harmonics and changes from beat to beat, and algorithms for beating-heart surgery were built on a model of the heart's motion and a measured biological signal such as the electrocardiogram [3]. Rules imposed on the robot's own command, forbidden regions and guidance paths, were surveyed in 2014 under the names active constraints and virtual fixtures [7].

Autonomy came last, and the second history segment below follows its first two steps on the bowel. Over the same decade robotic surgery spread from urology to the common procedures of general surgery, which a statewide study of hospitals traced from 2012 to 2018 [15]. Outcome work set clinical limits that a control engineer can read as budgets. In partial nephrectomy, each minute of warm ischemia with the renal hilum clamped was associated with a higher risk to the kidney's function [16], which is the reason for the clock of cases 9 and 12. The simulator puts these steps on one robot so that each can be tried alone or with the others.

> ⧖ HISTORY **The Robot Takes the Needle, 2016 and 2022**
>
> In 2016 a robot performed supervised autonomous surgery on soft tissue in living pigs, in an open surgical setting. A three-dimensional and near-infrared fluorescent imaging system tracked the tissue, a program planned the sutures of an intestinal anastomosis, and the outcomes were better than those of expert surgeons and of robot-assisted surgery in the tissues tested [8]. In 2022 the task was done laparoscopically, in pigs followed for a week afterward. The robot detected the breathing motion of the tissue and told the operator to start a replanning step, and the operator selected among suture plans the robot had generated. On the scale of autonomy that runs from pure teleoperation, level 0, to full autonomy, level 5, a system that generates strategies and relies on a human to select or approve one is level 3, conditional autonomy [17].

14.3 Instrument, Tissue and Patient as Simulated

The simulated platform is one docked teleoperated robot with a console, a wristed instrument driven by the surgeon's hand, a third arm that grasps and retracts tissue, and an endoscope, all through fixed ports, as shown in Figure 14.1. The frame is the endoscope's, with x to the right of the image, y up the image toward the head and z into the patient, and the operative surface lies at $z = 0$ in the organ's own frame, which the organ's motion carries. Every tissue property, limit, motion, latency and time budget is a teaching value, both the model dialog and the Instructions page label them so, and no number applies to any patient, instrument or product. Table 14.1 classifies the signals.

14.3.1 The Instrument Through Its Port

Each instrument is a rigid shaft through its port $\mathbf{p}_{port}$, with six joints, the shaft's pitch θ and yaw ϕ about the port, the insertion d from the port to the wrist, the roll ψ about the shaft, and a two-axis wrist with pitch α on a link $l_{w1} = 5\,\text{mm}$ and yaw β on a jaw $l_{w2} = 10\,\text{mm}$. The forward kinematics are shown in Equation (14.1).

$$\begin{aligned} R_s &= R_0\,R_y(\theta)\,R_x(\phi), \qquad \mathbf{s} = R_s\,\mathbf{e}_z \\ \mathbf{p}_w &= \mathbf{p}_{port} + d\,\mathbf{s} \\ \mathbf{p}_{tip} &= \mathbf{p}_w + R_s R_z(\psi) R_x(\alpha)\left(l_{w1}\mathbf{e}_z + R_y(\beta)\,l_{w2}\mathbf{e}_z\right) \end{aligned} \tag{14.1}$$

where R_0 is a fixed rotation that points the shaft's zero at the operative field. The shaft passes through the port by construction, so the remote center is a property of the joint coordinates rather than a constraint the integrator must hold. The application's tests check it anyway, on the integrated states of every case, from two independently written expressions of the shaft, and the worst distance from the port to the shaft line is zero within the 0.05 mm bound.

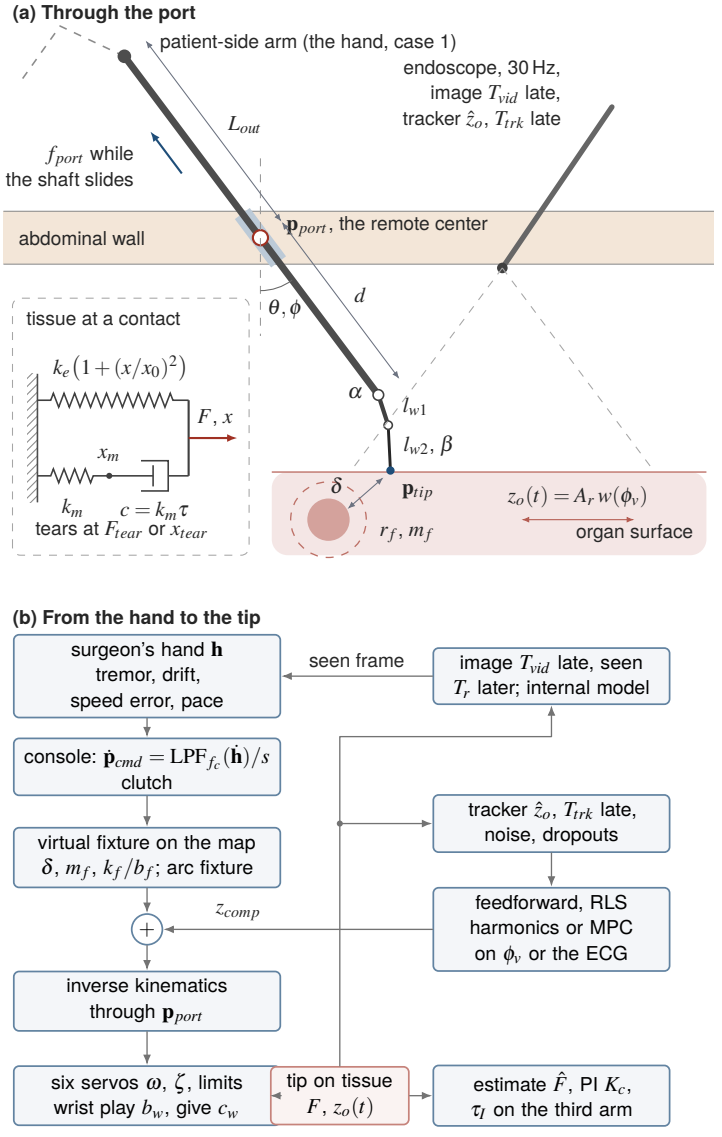


Figure 14.1 The instrument, the tissue and the control stack. (a) A section through the abdominal wall along the instrument, in the layout of the application's Port view. The shaft pivots by θ and ϕ about the port $\mathbf{p}_{port}$, a remote center that does not move, and slides by the insertion d. The wrist pitches by α on the link l_{w1} and yaws by β on the jaw l_{w2} to the tip $\mathbf{p}_{tip}$. Held by hand (case 1) the handle sits L_{out} outside the port. The organ moves by $z_o(t)$ on the ventilator's phase ϕ_v, a forbidden region of radius r_f and margin m_f lies at a distance δ from the tip, and the endoscope and the tracker see everything a latency late. The inset is the standard linear solid of every contact, with the equilibrium spring k_e, the Maxwell arm k_m and c with its internal state x_m, the stretch x and the force F. (b) The chain from the hand to the tip and the signals each controller reads. Not to scale.

Table 14.1 Signals by Role. Ranges Are Those the Interface Offers

Symbol	Role	Default	Range
$\mathbf{p}_{tip}$	CV, the tip in the task axis	—	—
$\mathbf{p}_{cmd}$	SP of the tip, from the console	—	—
$\hat{F}$	CV of the force loop (estimate)	—	—
F_{SP}	SP of the force loop	0.8 N	0.1 to 3.5 N
$\mathbf{h}$	MV, hand h_x, h_y, h_z (Manual)	0	±150 mm
x_s	MV, pull depth (Position)	4 mm	0 to 15 mm
$\mathbf{q}_c$	MV, six joint commands per arm	from IK	ranges
$\mathbf{q}$, $\dot{\mathbf{q}}$	states, 2×6 joints and rates	per case	ranges
x_m	states, three Maxwell arms	0	—
ϕ_h	state, the heart's phase	0	—
$\hat{z}_o$	measured, tracker report	100 ms late	40 to 200 ms
ϕ_v, t_R	measured, ventilator phase, ECG R wave	—	—
$\mathbf{q}$, $\dot{\mathbf{q}}$	measured, joint encoders	—	—
F, z_o	hidden, true force and organ	—	—
A_r	DV, respiration (peak to peak)	per case	0 to 20 mm
A_c, HR	DV, heart motion and rate	8 mm, 72 bpm	0 to 15 mm
—	DV, beat-to-beat variability	±5 %	0 to ±10 %
e_{reg}	DV, fixture registration error	0	±8 mm
—	DV, instrument age	0 %	0 to 100 %
f_{port}	DV, port friction	0.3 N	0 to 1 N
—	DV, tracker dropout (2 s)	—	event

The inverse takes a commanded tip, the jaw's commanded direction $\mathbf{u}$ and the roll, and returns the joints. The wrist angles follow in closed form from $\mathbf{u}$ in the shaft's frame, and the shaft's direction and insertion follow from where the wrist must then be. The two depend on each other only through the first wrist link, 5 mm against a shaft of 20 to 250 mm, so the fixed-point iteration of Equation (14.2) converges geometrically, at about the ratio of the link to the insertion.

$$\mathbf{s}^{(k+1)} = \frac{\mathbf{p}_2 - l_{w1}\,\mathbf{e}_1\big(\alpha(\mathbf{s}^{(k)})\big) - \mathbf{p}_{port}}{\big\|\mathbf{p}_2 - l_{w1}\,\mathbf{e}_1\big(\alpha(\mathbf{s}^{(k)})\big) - \mathbf{p}_{port}\big\|} \tag{14.2}$$

where $\mathbf{p}_2 = \mathbf{p}_{tip} - l_{w2}\mathbf{u}$ is the wrist's yaw joint and $\mathbf{e}_1$ is the direction of the first wrist link. Over 4000 random poses the worst case took 19 passes to 10^{-13} m, and the forward and inverse kinematics round-trip within 3×10^{-14} m. A sideways tip speed v needs a pivot rate of about v/d, so the pivots saturate as the tip comes back toward the port.

Case 1 has no robot. A straight instrument of 360 mm is held by its handle, which lies L_{out} outside the port on the line through the tip, and inside the port lie $L_{in} = 360\,\text{mm} - L_{out}$. A small lateral motion Δh of the handle moves the tip by Equation (14.3).

$$\Delta x_{tip} = -\frac{L_{in}}{L_{out}}\,\Delta h \tag{14.3}$$

At $L_{in} = 120$ mm the ratio is -0.500 and at 200 mm it is -1.250, the values the application's tests check. A 20 mm move gives 9.90 mm and 24.65 mm, a little less than the ratio because the handle swings on an arc about the port.

14.3.2 Joint Servos and the Cable-Driven Wrist

Every joint of both arms follows its command through the second-order servo of Equation (14.4), copied with its provenance from the six-axis arm of the shared framework, whose kinematic chain is a different structure.

$$\begin{aligned} \ddot{q}_i &= \mathrm{sat}_{a_{max,i}}\big(\omega^2(q_{c,i} - q_i) + 2\zeta\omega\,(\dot{q}_{ff,i} - \dot{q}_i)\big) \\ |\dot{q}_i| &\le v_{max,i}, \qquad q_{min,i} \le q_i \le q_{max,i} \end{aligned} \tag{14.4}$$

where $\omega = 2\pi \cdot 5\,\text{Hz}$, $\zeta = 0.8$, and the rate feedforward $\dot{q}_{ff,i}$ is the command's own difference over the 2 ms control period. The rate limits are 90 °/s on pitch and yaw, 0.2 m/s on insertion and 180 °/s on roll and the wrist, the acceleration limits are five times the rate limits per second, the shaft's angles stay within $\pm 70^\circ$, the wrist's within $\pm 90^\circ$ and the insertion between 20 and 250 mm. Approaching a range end, a drive starts to brake once stopping would need 80 % of its acceleration limit, and a hard stop after each step holds the range.

The wrist is driven by cables, so the jaw's delivered pitch differs from the servo's by a backlash and by a compliance under the load across the jaw, as shown in Equation (14.5).

$$\alpha_{tip} = \text{play}(\alpha, b_w) - \text{sign}(\dot{\alpha})\,\frac{c_w}{l_{w2}}\,F_t \tag{14.5}$$

where play is the play operator of half-width b_w, which grows linearly from 0.5° new to 3° at the end of the instrument's life, $c_w = 0.3\,\text{mm/N}$ is the give at the jaw's tip, and F_t is the needle's drag along its path. Both are applied once per control period as a kinematic offset, never inside the derivative function. The needle's point is 28 mm from the wrist's pivot, so one degree of play is about 0.5 mm at the point.

14.3.3 Tissue at the Contacts

Tissue is lumped at the points of contact. Each held or compressed tissue is a standard linear solid [9], an equilibrium spring that stiffens with stretch in parallel with a Maxwell arm, as shown in Equation (14.6).

$$\begin{aligned} F &= k_e\,x\big(1 + (x/x_0)^2\big) + k_m\,(x - x_m) \\ \dot{x}_m &= \frac{x - x_m}{\tau}, \qquad \tau = \frac{c}{k_m} \end{aligned} \tag{14.6}$$

where x is the stretch the instrument imposes and x_m the state of the Maxwell arm. Under a held stretch the force relaxes from the instantaneous stiffness $k_e + k_m$ toward k_e and loses the share $k_m/(k_e + k_m)$ of its linear part with time constant τ. Under a held force the stretch creeps with the longer time constant $\tau(k_e + k_m)/k_e$. A tissue tears when $F > F_{tear}$ or $x > x_{tear}$, tested after each step and latched. The bladder flap of case 4 has $k_e = 150\,\text{N/m}$, $k_m = 250\,\text{N/m}$, $\tau = 4\,\text{s}$, $x_0 = 15\,\text{mm}$, $F_{tear} = 3\,\text{N}$ and $x_{tear} = 10\,\text{mm}$, so a held stretch loses 0.625 of its linear force and a held force creeps with a time constant of 10.7 s. The flap's stretch is the third arm's travel from the grasp along the pull. The suture line under tension uses $k_e = 120$ and $k_m = 180\,\text{N/m}$, $\tau = 3\,\text{s}$, $x_0 = 6\,\text{mm}$ and $F_{tear} = 1.5\,\text{N}$. Bowel between the stapler's jaws uses $k_e = 300$ and $k_m = 600\,\text{N/m}$, $\tau = 15\,\text{s}$ and $x_0 = 2\,\text{mm}$, and the jaws close 3 mm of bowel to a gap of 1.5 mm in 3 s. The staple-line stress index is the force at firing over the force the same gap holds once fully relaxed.

A curved needle of radius $r_n = 7\,\text{mm}$, five eighths of a circle held 75° from its swage, follows a reduced form of the three phases of needle insertion [10]. The surface deflects ahead of the point up to $F_{pk} = 1.0\,\text{N}$ at 2 mm, the point punctures, and the shaft then drags $F_{fr} = 0.4\,\text{N}$. Any motion of the needle's center away from where it entered cuts the tissue sideways, as shown in Equation (14.7).

$$F_l = \frac{\|\Delta\mathbf{c}\|}{1/k_{lat} + c_w\left((r_n + l_{w2})/l_{w2}\right)^2} \tag{14.7}$$

where $\Delta\mathbf{c}$ is the center's departure and $k_{lat} = 600\,\text{N/m}$ is the tissue across the needle, in series with the wrist's give carried out to the needle's center. The bite tears when F_l exceeds the suture line's 1.5 N. A bite is scored on the larger of its entry and exit errors against the plan, six bites 3 mm apart and 3 mm deep. Vessels that must not be touched are capsules, a segment and a radius, pushing back at 400 N/m of penetration. A contact counts on entry and a force above 0.5 N is an injury, which latches and stops the run.

14.3.4 The Patient's Motion

The operative organ moves rigidly by $z_o(t)$ along a fixed direction, as shown in Equation (14.8).

$$\begin{aligned} z_{resp}(t) &= A_r\, w(\phi_v), \qquad \phi_v = 2\pi t / T_v \\ z_{card}(t) &= A_c\, \frac{c(\phi_h) - c_{lo}}{c_{span}}, \qquad \dot{\phi}_h = \frac{2\pi}{RR} \\ c(\phi) &= \textstyle\sum_{k=1}^{3} a_k \cos(k\phi + \vartheta_k) \end{aligned} \tag{14.8}$$

where the breath shape w rises over the first third of the cycle as a raised cosine (an inspiratory to expiratory ratio of 1:2) and returns over the rest as an exponential in the phase with rate 1.27 that reaches zero at the cycle's end, so w runs from 0 to 1 and A_r is the peak-to-peak motion. The kidney moves $A_r = 12\,\text{mm}$ every $T_v = 4\,\text{s}$, mostly along the image's y axis. The heart's harmonics have $a_k = (1, 0.45, 0.2)$ and $\vartheta_k = (0, 0.8, 1.9)$ rad, c_{lo} and c_{span} normalize the sum to a peak-to-peak of one, and $A_c = 8\,\text{mm}$ at 72 beats per minute. The interval RR of each beat is drawn uniformly within $\pm 5\,\%$ of the mean, and an R wave marks the start of each beat. The heart's phase is the one state of the motion.

14.3.5 What the Controllers Can Know

The endoscope captures a frame every $1/30$ s and shows it $T_{vid} = 80\,\text{ms}$ later. A tissue tracker reports the organ's displacement from the same frames with its own latency T_{trk} (100 ms by default), Gaussian noise of 0.2 mm per axis, and nothing while blood or smoke hides the surface. The tip force is not measured. The estimate is the drive's effort less the servo's own model, so it carries the friction the model does not know, as shown in Equation (14.9).

$$\begin{aligned} \hat{F} = \mathrm{LPF}_{20\,\text{ms}}\Big(& F + f_{port} \tanh\left(-\dot{d}/v_s\right) \\ & + f_{cab} \tanh\left(|\dot{\alpha}|/\omega_s\right) + n_F \Big) \end{aligned} \tag{14.9}$$

where $f_{port} = 0.3\,\text{N}$ is the port's Coulomb friction along the shaft, $f_{cab} = 0.15\,\text{N}$ the wrist cables', $v_s = 0.5\,\text{mm/s}$, $\omega_s = 0.05\,\text{rad/s}$ and n_F is Gaussian noise of 0.02 N, through a first-order filter of 20 ms. A shaft sliding outward reads high and one sliding inward reads low, and at rest the bias vanishes. Every controller reads a measurement packet with exactly fourteen fields, the frame shown now, the frame the surgeon perceives, the newest tracker report, the two force estimates, the joint encoders, the ventilator's phase, the last R wave and its interval, the stapler's jaw force and the occlusion flag. A test wraps the packet in a proxy and fails if a controller touches anything else, and the simulator's truth reaches only the scene and the 12 exported columns that begin with `truth_`.

14.3.6 The Scripted Surgeon

In Auto mode a scripted surgeon moves the hand toward the current target of a task script by a visuomotor loop on the frame shown $T_r = 180\,\text{ms}$ ago, itself 80 ms old. A position loop with 1 Hz of bandwidth through 0.26 s of dead time is unstable, by the delay margin of an integrating loop in Equation (1.16), so the surgeon carries an internal forward model of the tip motion they have intended, $\mathbf{I}(t)$, and judges the tip by Equation (14.10).

$$\begin{aligned} \hat{\mathbf{p}} &= \mathbf{p}_{seen}(t_{cap}) + \mathbf{I}(t) - \mathbf{I}(t_{cap}) \\ \dot{\mathbf{I}} &= \mathrm{sat}\big(K\,(\mathbf{p}_{target} - \hat{\mathbf{p}}),\; v_h\,\pi_s/s\big) \end{aligned} \tag{14.10}$$

where t_{cap} is the capture time of the frame the surgeon sees, $K = 2\pi\pi_s\ \text{s}^{-1}$ with the pace π_s (1 by default), s is the motion scale and $v_h = 0.15\,\text{m/s}$ is the hand's speed ceiling. The model covers the image's latency and the surgeon's own reaction and expects no lag from the robot. A slow tremor filter adds lag that the model does not know, and the surgeon pushes on toward a tip the image shows

Table 14.2 Model Parameters. A Is Adjustable in the Model Dialog, D a Disturbance, F Fixed in the Source

Symbol	Meaning	Value	
l_{w1}, l_{w2}	wrist link, jaw	5, 10 mm	F
$\omega/2\pi$, ζ	servo bandwidth, damping	5 Hz, 0.8	C
v_{max}	pitch and yaw, insertion, roll and wrist	90 °/s, 0.2 m/s, 180 °/s	F
c_w	wrist give at the jaw's tip	0.3 mm/N	A
b_w	wrist play, new to end of life	0.5 to 3°	D
k_e, k_m, τ	flap	150, 250 N/m, 4 s	F, A
x_0, F_{tear}, x_{tear}	flap	15 mm, 3 N, 10 mm	F, A, A
F_{exp}	tension the dissection needs (case 4)	0.7 N	F
—	suture line k_e, k_m, τ, F_{tear}	120, 180 N/m, 3 s, 1.5 N	F, A
—	bowel k_e, k_m, τ	300, 600 N/m, 15 s	F, A
F_{pk}, F_{fr}, k_{lat}	needle peak, drag, lateral	1.0 N, 0.4 N, 600 N/m	F, F, A
r_n	needle radius	7 mm	F
—	vessel contact stiffness, injury	400 N/m, 0.5 N	F
A_r, T_v	kidney motion, ventilator period	12 mm, 4 s	D
A_c, HR	epicardial motion, heart rate	8 mm, 72 bpm	D
T_{vid}, T_r	video latency, reaction	80 ms, 180 ms	A, F
T_{trk}	tracker latency	100 ms	D
—	tracker noise per axis	0.2 mm	F
f_{port}, f_{cab}	port, cable friction in $\hat{F}$	0.3 N, 0.15 N	D, F
K, v_h	surgeon gain, hand speed	2π s^{-1}, 0.15 m/s	F
—	tremor, drift, speed error	0.3 mm, 0.7 mm, 8 %	F
Δt	physics and control step	2 ms	F

C: a setting on a control card. The servo, the flap's relaxation time and both tear forces, the bowel's relaxation time and the lateral stiffness are on the model dialog. Every value is a teaching value.

short of its target. The hand then moves s times the intended tip motion with three imperfections, a tremor of 0.3 mm RMS from a resonator at 10 Hz with a damping ratio of 0.2 (a half-power band of 8 to 12 Hz), a drift of $0.7\,\text{mm}\,\pi_s$ RMS with a 1 s correlation time, and a speed error of $8\,\%\,\pi_s$ with a 0.1 s correlation time. A needle drive rotates the hand's wrist at $1.2\,\text{rad/s}\,\pi_s$ and makes 60 % of the translation the rotation needs. On a breathing organ the surgeon starts each drive in the quiet tail of expiration, read from the ventilator's phase. In Manual mode the hand follows the student's sliders or arrow keys at up to 0.15 m/s and carries the same tremor from the same generator. The surgeon's parameters are illustrative and describe no surgeon.

14.3.7 Parameters and Numerics

A fourth-order Runge–Kutta step of 2 ms integrates the physics (Section 1.6.1), the console, the inverse kinematics and the force loop run every 2 ms, the surgeon and the tracker at the 30 Hz frame, and model predictive control every 10 ms. The 28 continuous states are the six joints and rates of each arm, the three Maxwell arms and the heart's phase. Everything discrete happens after the integration, in this order, the joint stops, the hand-held lever of case 1, the wrist's offsets, the needle's puncture, exit, tear and hand-off, vessel contacts, incursions, the flap's tear and slip, the stapler, the R waves, the dropouts and the ischemia clock. Halving the step keeps the conclusions of cases 3, 6 and 8. Every random draw comes from its own seeded stream, so a case replays bit for bit after Reset. Headless, the model runs 24 000 steps per second with model predictive control on case 8 and 166 000 on case 1, and in Chrome the eight-minute challenge keeps 20 × real time while drawing. The parameters are listed in Table 14.2.

14.3.8 Assumptions

The joints are servo-level, with no rigid-body dynamics, so a contact force moves the instrument only through the wrist's give. A real arm's inertia and its own controller would add lag and coupling that matter faster than the 5 Hz servo. One instrument and the third arm are simulated, while the endoscope, the second instrument and the patient-side arms are drawn. The needle's hand-off to the second instrument and its return between bites are timed steps. The ports are fixed remote centers,

Table 14.3 Controller Settings, Defaults and Ranges. Cases Ship Their Own Values Where Stated

Symbol	Setting	Default	Range
s	motion scale, hand to tip	3	1, 2, 3, 5
f_c	tremor filter cutoff	6 Hz	1 to 30 Hz
—	clutch	engaged	released
π_s	scripted surgeon's pace	1.0	0.5 to 2.0
K_c	force loop gain	10 mm/s per N	1 to 50
τ_l	force loop reset time	2 s	0.2 to 20 s
F_{max}	force ceiling	2.0 N	0.2 to 5 N
—	force loop mode	Force	Position
k_f	fixture stiffness (adv.)	2000 N/m	200 to 5000
—	virtual fixture, arc fixture	off, on	on, off
—	motion compensation	none	ff, adaptive, MPC
N_h	harmonics	3	1 to 5
λ	forgetting factor	0.99	0.95 to 0.999
—	autonomy, map	off, tracked	run or halt, perfect
t_w	wait before firing	0 s	0 to 60 s

and the abdominal wall's breathing is drawn around them rather than applied, which ignores the force the wall puts on the cannula. Tissue is lumped at the contacts, so strain is not redistributed, a tear has no location and a needle does not steer. The needle is driven by pitching the jaw in the wrist's plane, where a real needle driver rolls it. The organ moves as a rigid body with no deformation, the tracker sees that displacement only, and the ECG gives the heart's phase from its R waves alone. There is no haptic channel to the hand, no bleeding and no smoke beyond the tracker's dropouts. Each simplification keeps the one-dimensional mechanism a lesson needs and leaves out what would decide a real operation.

14.4 The Controllers as Coded

Every 2 ms the controller builds the measurement packet, moves the hand, applies the console, the fixtures, the autonomy, the force loop and the compensation, and solves the inverse kinematics, in that order. Its settings are listed in Table 14.3.

14.4.1 The Console

The console differentiates the hand over the control period, filters the velocity with a second-order Butterworth low-pass and divides it by the scale, as shown in Equation (14.11).

$$\mathbf{p}_{cmd,k} = \mathbf{p}_{cmd,k-1} + \frac{\Delta t}{s}\,\mathrm{LPF}_{f_c}\!\left(\frac{\mathbf{h}_k - \mathbf{h}_{k-1}}{\Delta t}\right) \tag{14.11}$$

The filter is discretized by the bilinear transform with the cutoff prewarped, so its −3 dB point is exactly f_c, and it passes $1/\sqrt{1+(f/f_c)^4}$ of a component at f. At 6 Hz it passes 0.339 of a 10 Hz tremor and delays a 1 Hz motion by 37.9 ms, and at 2 Hz it passes 0.040 and delays the same motion by 120.3 ms (the group delay is 132.4 ms). Scaling the velocity rather than the position means that releasing the clutch, recentering the hand and engaging again does not move the tip. The needle's rotation follows the hand's wrist one to one through the same filter.

14.4.2 Virtual Fixtures

A forbidden region is a capsule of radius $r_f = 8$ mm around a structure, with a margin $m_f = 6$ mm, placed where the map says the structure is. The fixture acts on the command increment $\Delta\mathbf{p}$, as shown in Equation (14.12).

$$\begin{aligned} \Delta p_\perp &\leftarrow \Delta p_\perp \,\mathrm{clamp}(\delta/m_f, 0, 1) \\ \mathbf{p}_{cmd} &\leftarrow \mathbf{p}_{cmd} - \delta\,\hat{\mathbf{n}}\,\min\!\left(1, (k_f/b_f)\,\Delta t\right) \end{aligned} \tag{14.12}$$

where δ is the command's distance to the edge of the registered region, $\Delta p_{\perp}$ the part of the increment toward the region (scaled only when it is positive), the second line acts only while $\delta < 0$, $\hat{\mathbf{n}}$ is the outward normal, and $k_f / b_f = 2000/40 = 50\,\mathrm{s}^{-1}$. A registration error moves the region on the map, not in the patient, and the audit counts incursions against the true region, the check against the truth of Section 1.4.9. During a needle drive, the arc fixture replaces the command with the point that keeps the needle's center where the drive began, so the jaw turns about the needle's own center whatever the hand translates.

14.4.3 The Force Loop

The third arm's retraction in case 4 and the needle driver's suture pull run on the shared velocity-form law of Section 1.6.2, with only the emitted output clamped. In this loop's symbols it is Equation (14.13).

$$\begin{aligned} e_k &= F_{SP} - \hat{F}_k \\ v_k &= \mathrm{clamp}\big(K_c\, e_k + I_k,\ -v_{lim},\ v_{up}\big) \\ I_{k+1} &= I_k + \Big[\frac{K_c}{\tau_I}\, e_k + \frac{v_k - (K_c e_k + I_k)}{\tau_I}\Big]\Delta t \end{aligned} \tag{14.13}$$

where v is the arm's pull velocity along the retraction direction, $v_{lim} = 5\,\mathrm{mm/s}$, and v_{up} is 5 mm/s below the force ceiling and 0 above it, so the loop never pulls harder once the estimate exceeds the ceiling. The loop is reverse acting in the convention of Section 1.3 ($a = +1$), because a larger pull raises the force. The derivative is off, back-calculation anti-windup uses a tracking time constant equal to τ_I, and the sample period is 2 ms. Because the loop sets a pull velocity, its proportional term is the integral force law of Section 1.4.8 acting on the pull depth, here through tissue that relaxes, and Chapter 13 closes the same kind of loop on a measured force at a peg. In Position mode the arm approaches the station's depth at 5 mm/s while the law tracks it, so a switch in either direction is bumpless. The loop acts on the biased estimate of Equation (14.9), never on the true force. A suture pull is done when the estimate has held within 0.1 N of its setpoint for 0.8 s, or after 4 s.

14.4.4 Motion Compensation

Each compensation option adds an offset $\mathbf{z}_{comp}$ to the command so that the surgeon works in the organ's frame. Ventilator feedforward fits, per axis, a gain and an offset by least squares to the tracker's reports over the last breath, on a template that knows the ventilator's inspiratory to expiratory ratio but not the patient's exhalation (a raised cosine up and a raised cosine down, where the organ in fact returns exponentially). The adaptive harmonic predictor fits, per axis, a truncated Fourier series of the phase, as shown in Equation (14.14).

$$\hat{z}(\phi) = c + \sum_{k=1}^{N_h} \big(a_k \cos k\phi + b_k \sin k\phi\big) = \theta^{\mathsf{T}} \varphi(\phi) \tag{14.14}$$

Its coefficients are updated on each tracker report, at the phase the report was captured, the correction for report age of Section 1.4.6 applied to a phase. Chapter 10 moves each camera report on by the belt travel since its capture in the same spirit. The update is recursive least squares with forgetting written in symmetric form, as shown in Equation (14.15).

$$\begin{aligned} \mathbf{k} &= \frac{P\varphi}{\lambda + \varphi^{\mathsf{T}} P \varphi}, \qquad \theta \leftarrow \theta + \mathbf{k}\,(\hat{z}_o - \theta^{\mathsf{T}}\varphi) \\ P &\leftarrow \frac{1}{2\lambda}\Big[(P - \mathbf{k}\varphi^{\mathsf{T}} P) + (P - \mathbf{k}\varphi^{\mathsf{T}} P)^{\mathsf{T}}\Big] \end{aligned} \tag{14.15}$$

with $P_0 = 10^4 I$. With forgetting, the rounding error's antisymmetric part grows by $1/\lambda$ each report, and the textbook update lost positive definiteness after about 2500 reports at $\lambda = 0.99$ and diverged in the challenge. The forecast is evaluated at the phase of $t + 50\,\mathrm{ms}$, past the servo's lag, so the offset

lands where the organ will be when it reaches the tip. The ventilator's phase is exact. The heart's is taken from the ECG as $\phi = 2\pi \min\left(1.25, (t - t_R)/RR_{last}\right)$, so a beat longer or shorter than the last is a phase error that no report can reveal until the next R wave. A model is trusted after one whole cycle of reports and blends in over 0.5 s.

The model predictive option runs the shared linear model predictive controller of Section 1.6.3 on a double integrator per axis, the offset and its rate driven by an acceleration, every 10 ms over a 0.5 s horizon of 50 steps with graduated move blocking. It tracks the adaptive forecast with a weight of 1 on the offset, 10^{-6} on moves and 10^{-8} on the input (in millimeters), keeps the acceleration inside $0.8\,a_{max}\,d$ and the rate inside a soft band of $0.8\,v_{max}\,d$ (what the shaft's pivots can add at the present insertion), and integrates the planned acceleration between solves. On a failed solve the adaptive offset takes over bumplessly, and the option is labeled MPC only while the optimization ran. The supervisor's watchdog freezes every offset when the tracker has reported nothing valid for 0.1 s, lets it decay linearly to zero over 2 s, stops the models' learning and blends back onto the forecast over 0.5 s when the track returns.

14.4.5 Supervised Autonomous Suturing

In case 10 a planner, a tracking controller and a supervisor replace the hand. The planner places six bites 3 mm apart and 3 mm deep from the tracked tissue edges, each point carrying the edge finder's seeded error of 0.15 mm. The controller moves the jaw to the approach pose by a minimum-jerk blend $\sigma(\tau) = 10\tau^3 - 15\tau^4 + 6\tau^5$ over 1.2 s, the quintic of Section 1.4.4, rotates the needle about its own center through the bite over 1.6 s, waits 0.8 s for the hand-off, carries the suture to 4 mm above the exit, pulls it with the force loop to 0.5 N and releases. The supervisor halts on a lost track, an estimated force over its 1.6 N ceiling, tissue more than 2 mm from where the plan was made, or the student's Halt, and the motion brakes along its own path over 0.25 s. Freezing the command instead let the fast wrist overrun by about 7° and swing the point 3 mm sideways into the tissue. It resumes only on the student's Run, after replanning the remaining bites. A stage sequencer from the shared framework keeps the ledger, one stage per bite.

14.4.6 Three Models

Section 14.3 is the simulation model, and the controllers' internal models are much smaller. The inverse kinematics knows the chain exactly but not the wrist's play or give, the force loop has no model of the tissue, the predictor's model is a truncated Fourier series of the phase, the model predictive controller's is a double integrator, and the surgeon's is a forward model of their own motion with no robot lag. No model is identified from data. The simulated truth is logged beside every estimate for the audit. The latched injury stop and the out-of-view warning are judged on that truth, while every decision a controller makes is taken on the packet.

14.5 Twelve Cases, Measured

The eleven cases are excerpts of a few minutes from robot-assisted operations, the general surgical ones among the procedures whose move to the robot a statewide study traced [15], each at the step where one control element decides the outcome, and the challenge combines them, as listed in Table 14.4. Each result below was measured headlessly at the case's default seed with the scripts named in the application's build record, and the outcomes are collected in Table 14.5.

> **+ DID YOU KNOW? Robotic Surgery's Rapid Spread**
>
> In a statewide registry of 73 hospitals, the share of general surgery procedures done with a robot rose from 1.8 % in 2012 to 15.1 % in 2018. For inguinal hernia repair, the step of case 5, it rose from 0.7 % to 28.8 % [15].

Table 14.4 The Eleven Cases and the Challenge

#	Procedure and step	Control element
1	Cholecystectomy, the instrument by hand	the fulcrum, Equation (14.3)
2	Cholecystectomy, through the robot	inverse kinematics, rate limits near the port
3	Cholecystectomy, Calot's triangle	scaling against tremor, filter lag
4	Hysterectomy, holding the bladder flap	relaxation, creep, a force loop on an estimate
5	Inguinal hernia, the triangle of doom	a virtual fixture and its registration
6	Prostatectomy, the anastomosis	the needle's arc, the wrist's play and give
7	Colectomy, the stapler	the wait before firing
8	Partial nephrectomy, the breathing kidney	feedforward, adaptive, MPC, a dropout
9	Partial nephrectomy, the clock	pace against an ischemia budget
10	Small-bowel anastomosis, the robot sutures	a planner and a supervisor that halts
11	Coronary bypass on a beating heart	an infeasible rejection
12	Challenge, a renorrhaphy within 25 min	all of them on one seed

Table 14.5 Outcomes Read From the Running Engine, Default Seed

#	Setting	Outcome
2	tip at 29.4 mm insertion, 60 mm move	pitch at 90 °/s for 0.56 s, tip up to 51.5 mm behind
3	1:1, 30 Hz / 3:1, 6 Hz / 3:1, 2 Hz	6 / 0 / 3 artery contacts, tremor at the tip 111 / 31 / 12 µm
4	Position, 4 mm	peak 1.64 N, slip at 11.5 s, 0.64 N at 120 s
4	Force 0.8 N / 2.0 N / 2.5 N	creeps to 4.83 mm / 9.51 mm at 120 s / tears at 13.3 s
5	fixture off / on / +4 mm / −4 mm	1 / 0 / 2 / 0 incursions, 8.6 s blocked at −4 mm
6	new / end of life / no arc fixture	bites 0.29–0.73 / 0.69–1.60 and one missed / up to 1.47 N across
7	wait 0 / 15 / 30 / 45 s	stress index 2.24 / 1.46 / 1.17 / 1.06
8	none / ff / adaptive / MPC	3.29 / 2.19 / 1.10 / 1.13 mm RMS, 10–90 s
9	pace 0.6 / 1.0 / 1.4 / 1.8	over / 22.15 / 20.82 / over 25 min
10	tracked / perfect map	halt 62 ms after the dropout / no halt, bites 0.32–0.74 / 0.32–0.40 mm
11	none / ff / adaptive / MPC, 100 ms	3.86 / 3.22 / 1.71 / 1.57 mm RMS
12	shipped / suggested	clamp on at 25 min, 13 incursions, 9 tears / off at 22.1 min, none

14.5.1 The Fulcrum and Its Inversion

Held by hand in case 1, the instrument reverses and scales the hand's motion as Equation (14.3) says, and the hand's tremor goes through the same lever. At rest the tip carries 107 µm RMS of it in the 8 to 12 Hz band. Case 2 puts the same instrument on the robot at one to one with a 30 Hz filter, and a 20 mm hand move carries the command 20.5 mm with the tip within 1.53 mm of it, the tremor the filter lets through. With the tip brought back to 29.4 mm of insertion, a 60 mm hand move drives the shaft's pitch to its 90 °/s limit for 0.56 s, and the tip falls up to 51.5 mm behind its command before it catches up. At 105 mm of insertion the same limit allows 165 mm/s at the tip, and at 30 mm only 47 mm/s. The inversion is exact, and the limits are the joints'.

14.5.2 Scaling Against Lag

In case 3 the scripted surgeon clears the tissue in Calot's triangle with eleven strokes of 6 mm toward the cystic artery, each ending 1.45 mm from its wall. At one to one with a 30 Hz filter the hand's tremor and drift reach the tip whole, the artery is touched six times, the deepest 0.08 mm into the wall, and the strokes take 80.9 s because the tip will not settle. At 3:1 and 6 Hz nothing touches, the closest approach is 0.49 mm outside the wall, and the strokes take 35.9 s. At 3:1 and 2 Hz the tremor at the tip falls to 12 µm, but three strokes reach the artery, the deepest 0.95 mm in. The cause is the lag the surgeon's forward model does not contain. With the tremor, drift and speed error switched off, a single 6 mm stroke at 3:1 overshoots by 0.40 mm at 6 Hz and by 1.76 mm at 2 Hz, which is more than the 1.45 mm the stroke leaves. At 20 Hz the tip carries 50 µm of tremor against 31 µm at 6 Hz and still touches nothing. Over ten seeds the contacts are 2 to 7 at one to one, none at 3:1 with 6 Hz and 3 to 8 at 2 Hz, and none reaches the 0.5 N of an injury.

> **TRY IT IN THE APP** **3 · Cholecystectomy: Calot's Triangle**
>
> Press Run as shipped and count the artery contacts on the scorecard: six at one to one. Press Reset, set Motion scale to 3:1 and Tremor filter cutoff to 6 Hz, and run again: none. Press Reset and lower the cutoff to 2 Hz. The tremor at the tip falls to 12 µm, yet three strokes reach the artery.

Pause. Try Exercise 14.1 before reading on.

14.5.3 Tissue That Relaxes, Creeps and Tears

The third arm of case 4 pulls the bladder flap 4 mm and holds that position while the surgeon dissects, and the dissection needs 0.7 N of tension. The force peaks at 1.64 N, falls to 0.67 N at 15 s and settles at 0.64 N, what the equilibrium spring holds, so the flap slips at 11.5 s. The force loop at 0.8 N holds the estimate at its setpoint but walks the arm out as the tissue creeps, from 3.61 mm of stretch at 10 s to 4.83 mm at 120 s. While it walks the shaft slides outward, and at 10 s the estimate reads 0.807 N against a true 0.736 N, the port's friction acting on the loop. Early in the walk the true force sags just below the 0.7 N the dissection needs, and the scorecard counts one slip. From 60 to 120 s, with the arm nearly still, the estimate and the truth both average 0.800 N. At 2.5 N the stretch creeps past the 10 mm at which the flap tears, at 13.3 s, with the force 0.5 N below its tear force. At 2.0 N it creeps to 9.51 mm in 120 s and holds. A position hold fails slowly by relaxation and a force hold fails slowly by creep, and neither failure is visible in the force a loop regulates.

Pause. Try Exercise 14.2 before reading on.

The stapler of case 7 closes on the colon at 10 s and fires after the wait the student sets. Fired at once it meets 1.57 N, a stress index of 2.24 against the 0.70 N the same gap holds once relaxed. After 15, 30 and 45 s the index is 1.46, 1.17 and 1.06. The first relaxation time removes most of the excess, and every later second buys less.

14.5.4 Rules on the Command

In case 5 the surgeon raises the peritoneal flap along a path that passes 6 mm from the axis of the iliac vessels, inside the 8 mm region nothing may enter. With the fixture off the tip enters once, 2.44 mm deep. With it on the tip is turned aside at the edge, 8.02 mm from the axis. Registered 4 mm away from the dissection, the fixture admits the path, and the tip enters twice, 1.93 mm deep, with the fixture on. Registered 4 mm toward it, nothing enters, but the fixture holds the tip in safe tissue for 8.6 s, 11.79 mm from the axis. A fixture is as good as the map it is registered to, and its error appears either as an incursion or as safe motion blocked.

Pause. Try Exercise 14.3 before reading on.

The anastomosis of case 6 places six bites with the arc fixture on. With a new instrument the bites land 0.29 to 0.73 mm from their marks, and the needle carries at most 0.60 N across it from the wrist's give under the needle's drag. At the end of the instrument's life the 3° of play turns the needle about the wrist, the first bite's point never comes out of the tissue, and the rest land 0.69 to 1.60 mm off. Without the arc fixture a hand that turns a needle also pushes it, and the needle cuts sideways with up to 1.47 N across it, just under the 1.5 N that tears this tissue. At seeds 7 and 99 one bite tears.

14.5.5 The Patient's Motion

In case 8 the surgeon holds the tip on a mark on a kidney that moves 12 mm every 4 s, with a tracker 100 ms late that loses the kidney for 2 s at 60 s. From 10 to 90 s the hand alone holds the tip 3.29 mm RMS from the mark, ventilator feedforward 2.19 mm, the adaptive predictor 1.10 mm and model predictive control 1.13 mm. Feedforward knows the ventilator but not the exhalation. Three harmonics leave 0.35 mm of the breath's shape unexplained (five leave 0.20 mm), and model predictive control is no better than the predictor it tracks because at this insertion its rate and acceleration limits never bind, over 9000 solves with none failed. During the dropout every option freezes its offset and lets

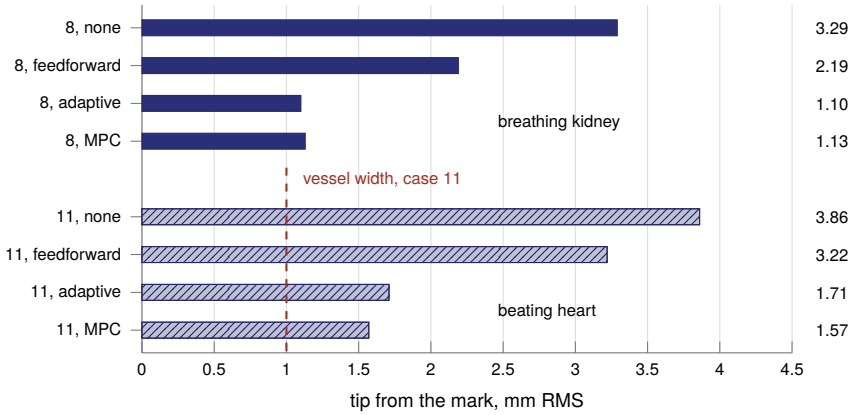


Figure 14.2 Distance of the tip from the mark under the four motion compensation options, from Table 14.5: the breathing kidney of case 8 (solid bars) and the beating heart of case 11 (hatched bars), default seed. Notice that learning the motion's shape cuts the kidney's error from 3.29 to 1.10 mm, while on the heart no option reaches the dashed width of the vessel.

it decay, and from 60 to 64 s the error is 3.43 to 3.48 mm RMS whatever the option, up to 6.87 mm. Figure 14.5 shows the organ one second into the dropout, with the compensation frozen.

> **TRY IT IN THE APP** **8 · Partial Nephrectomy: The Breathing Kidney**
>
> Load the case, keep Motion compensation at None and press Run. Watch the organ panel of the Console view: the hand chases the kidney late, and the tip holds 3.29 mm RMS from the mark. Press Reset, choose Adaptive harmonic and run again. The error falls to 1.10 mm, and at 60 s the offset freezes and decays while smoke hides the kidney.

The tracker's latency barely matters, as shown in Figure 14.3. From 40 to 200 ms the adaptive predictor on the kidney moves from 1.09 to 1.11 mm, because the forecast is evaluated on the ventilator's phase and the latency only delays which reports it has learned from. On the beating heart of case 11 the hand alone is 3.86 mm RMS from the vessel, feedforward 3.22 mm, the adaptive predictor 1.71 mm and model predictive control 1.57 mm, with the tracker 100 ms late. At 40 ms the best is 1.61 mm and at 200 ms 1.53 mm, and with no beat-to-beat variability model predictive control reaches 1.44 mm. No setting comes within the 1 mm width of the vessel, so the case is infeasible as declared. The motion repeats in 0.83 s, its third harmonic is at 3.6 Hz, close to the 5 Hz servo, and a beat 5 % longer than the last is a phase error of up to 18° that no forecast sees before the next R wave. Surgeons answer the heart with a stabilizer that holds a patch of it still, or by stopping it. Figure 14.2 draws the four options on both organs.

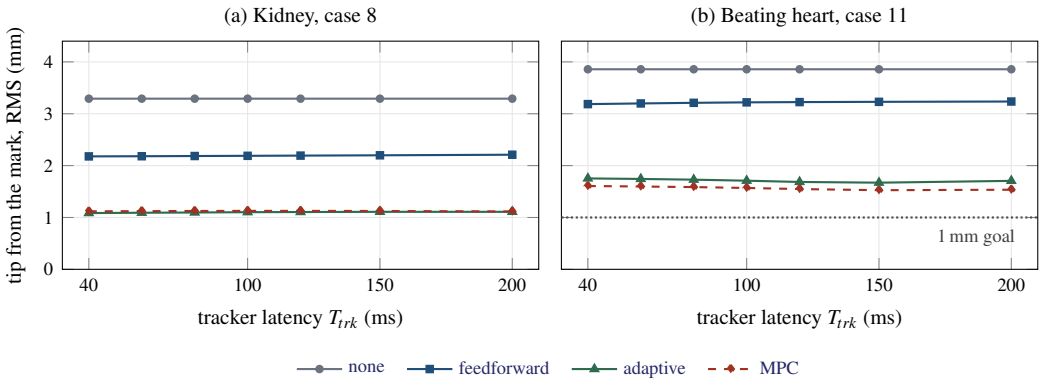


Figure 14.3 Tip distance from the mark against the tracker's latency, default seed. (a) The breathing kidney of case 8, RMS from 10 to 90 s with the 2 s dropout at 60 s. (b) The beating heart of case 11, RMS from 5 to 60 s, with the 1 mm width of the vessel dotted.

Table 14.6 Error Budget of the Hold on the Breathing Kidney, Case 8, Five Seeds. Mean-Square Error in mm^2

	No compensation		Adaptive	
Term	MSE	Share	MSE	Share
Motion alone (M)	1.735	17 %	0.237	18 %
Delay × motion (DM)	8.797	86 %	0.774	60 %
Hand alone (H)	0.057	1 %	0.057	4 %
Hand × delay (HD)	0.078	1 %	0.079	6 %
Instrument, all its terms	−0.449	−4 %	0.122	9 %
All other terms	0.016	0 %	0.022	2 %
Total (RMS)	10.234 (3.20 mm)		1.291 (1.14 mm)	

OPEN CHALLENGE **Holding a Tool on a Moving Organ**

Telerobotic systems that follow organs moved by breathing and the heartbeat have been developed for twenty years, and their potential for this work remains largely unexploited. Guidance by images alone suffers when landmarks are hidden, when the tissue deforms under the tool, and when the organ's motion makes the force fed back to the surgeon oscillate [18]. Progress would be a compensator that holds a tool on a beating heart within the width of a vessel, and keeps doing so while its tracker is briefly blind.

14.5.6 An Error Budget

Four sources of tip error were switched on and off in a two-level full factorial on the running engine, over the default seed and seeds 7, 99, 1 and 2. They are the hand (H, its tremor, drift and speed error, removed by setting all three to zero), the visuomotor delay (D, the 80 ms of video and the 180 ms of reaction, removed by setting both to zero, leaving the 30 Hz frame), the instrument (W, the wrist's give and half its life's play, removed to no give and the 0.5° of a new wrist), and the organ's motion (M, the 12 mm breath). The mean-square error pooled over the seeds is split exactly into a term for every subset of sources by Möbius inversion over the 16 cells, so a main effect is what a source costs alone and an interaction is what sources cost together beyond their sum. The decomposition of case 8's hold is listed in Table 14.6.

The delay costs nothing on a still mark (0.00 mm RMS with it alone), and the motion alone, with an instant visuomotor loop, costs 1.32 mm. Together they cost 3.25 mm, and their interaction is 86 % of the mean-square error. The surgeon's forward model covers the surgeon's own motion and not the organ's, so a target that moves is chased a quarter of a second late. The adaptive predictor cuts that

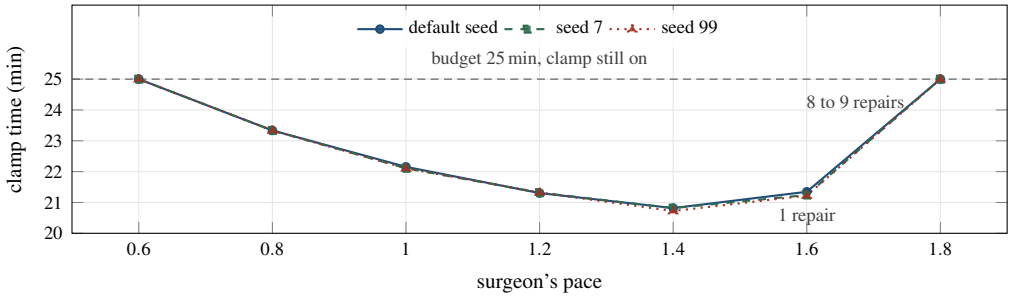


Figure 14.4 Warm ischemia time against the scripted surgeon's pace, case 9, at three seeds. A run still clamped at the 25 min budget is plotted at the budget. One repair appears at a pace of 1.6 and eight or nine at 1.8.

interaction from 8.797 to 0.774 mm^2, by 91 %, and the motion's own term from 1.735 to 0.237, by 86 %, while the hand's terms are unchanged at 0.057 and 0.078 mm^2, because scaling and filtering, not compensation, are what act on the hand. Over the five seeds the full hold is 3.18 to 3.22 mm RMS without compensation and 1.11 to 1.17 mm with it. With the instrument new, as case 8 ships, the pooled hold without compensation is 3.27 mm. In a hold the wrist carries no load, and its terms are small and of either sign.

> ✦ DID YOU KNOW? **A Delay That Costs Nothing Until the Organ Moves**
>
> From the simulator: on a still mark the surgeon's visuomotor delay costs nothing. On the breathing kidney its interaction with the motion is 86 % of the hold's mean-square error, and the adaptive predictor cuts that term from 8.797 to 0.774 mm^2 (Table 14.6).

The same factorial on case 6's six bites on still tissue, with the arc fixture on, gives a pooled 0.78 mm RMS, of which 0.37 mm remains with every source removed. Of the 0.612 mm^2, the instrument's four terms are 0.339 (55 %), the hand 0.072 and the delay 0.048, and with the half-worn wrist 3 to 5 of the 30 bites in each of its cells miss or tear. On the breathing kidney of case 9's renorrhaphy, with the clips and repairs switched off, no compensation leaves not one of the 240 bites placed by the eight cells with motion kept, whatever else is removed. With the adaptive predictor and every source present the pooled error is 1.19 mm with 3 of 30 bites missed or torn. There the terms are as large as the main effects and change sign. Removing the delay alone raises the pooled error to 1.86 mm with 12 bites lost, a mechanism the factorial did not isolate, so a single-source attribution does not hold for bites on a moving organ.

14.5.7 Pace Against the Clock

In case 9 the renal artery has been clamped for 17 of a 25 min budget, six renorrhaphy bites remain, each secured with a clip of 40 s, and a bite that tears, misses or lands more than 1.5 mm off costs 30 s and a new bite. The clamp time is shown against the pace in Figure 14.4. At 0.6 the clamp is still on at 25 min, at 1.0 it comes off at 22.15 min, at 1.4 at 20.82 min, and at 1.8 the surgeon makes nine repairs and overruns again. The optimum is interior at all three seeds, 20.72 to 20.82 min at a pace of 1.4. The loss index of the scorecard is a declared teaching curve, $e^{0.05(t-25)}$ with t in minutes, and the budget comes from the clinical finding that every minute of warm ischemia counts [16], not from any threshold that study states.

14.5.8 The Robot Sutures

In case 10 the robot closes an enterotomy by itself with the tracker 50 ms late. At bite 4 (23.42 s) the tracker loses the bowel, and the supervisor halts 62 ms later, braking along the path. When the student



Figure 14.5 The breathing kidney of case 8 with the adaptive harmonic predictor, at $t = 61.0$ s, one second into the tracker's 2 s dropout, on the Console view, cropped to the plant view. (1) The badge row, with the track lost and the compensation frozen. (2) The hand, scaled, against the command and the true tip (dashed). (3) The organ panel shows the true motion (dashed) leaving the tracker's last report while the frozen offset decays, and the tip is 6.31 mm from its mark. (4) The supervisor's state and the latencies it works with. (5) The status line.

sets the autonomy back to Run, three seconds later in the measured run, it replans and finishes the last bite at 47.0 s. The six bites land 0.32 to 0.74 mm from their marks, spaced within 0.19 mm of 3 mm. Each suture is pulled until the estimate reads 0.5 N, while the true tension is 0.28 N, the port's friction once more acting on the loop. The perfect map, a labeled teaching comparison, never halts and places every bite 0.32 to 0.40 mm off, the error that belongs to the instrument itself.

14.5.9 A Renorrhaphy Within the Budget

The challenge is a renorrhaphy on the breathing kidney with the hilum below the defect, an instrument at half its life, a 2 s dropout at 150 s and the clamp on for 17 of 25 minutes, and it ships at one to one, 30 Hz, no compensation, no fixture and a pace of 1.5. The target is the clamp off within 25 min with no hilum incursion, no tear, no stop and six kept bites within 1.5 mm. As shipped the surgeon chases the kidney, the bites land off and tear, the tip strays into the hilum's region 13 times, and after seven repairs the clamp is still on at 25 min, with 10 and 17 incursions at seeds 7 and 99. The suggested configuration (adaptive compensation, the fixture on, 3:1, 6 Hz and a pace of 1.2) takes the clamp off at 22.1 min with no incursion, no tear and the worst kept bite 1.46 mm off, and passes at seeds 7 and 99 at 22.1 and 23.2 min. At a pace of 1.0 the same settings overrun at seed 7, where two bites need repairs. The bite tolerance is 1.5 mm rather than 1 mm because the wrist's give, a half-worn wrist and the predictor's residual put most bites at the suggested settings beyond 1 mm.

14.6 Technology in Practice

The robot of Section 14.3 reads joint encoders, an endoscope, a tissue tracker and a force it estimates, and it moves the tip through joint servos and a cable-driven wrist. Figure 14.6 draws its loops with real devices in the place of the schematic's symbols.

What Measures It

Research systems find the organ by tracking markers or the tissue's surface in the endoscope's view, and they detect the breathing motion from it [17]. The tracker of Section 14.3, 100 ms late with 0.2 mm of noise and silent while blood or smoke hides the surface, stands for such a tracker. The force at the tip is harder to measure. Sensors at the tip face severe limits of size, geometry, cost, biocompatibility and sterilization, so the force would ideally be estimated without them. On a robot with low inertia and friction, the gap between the commanded and the actual position indicates the force, but the robot's own dynamic forces often mask the small forces of tissue [13]. A tension read near the motors carries the friction of the cables [19]. The estimate of Equation (14.9), biased by the port's and the cables' friction, stands for this kind of measurement.

> **TECHNOLOGY** **Sensor: Tracking Tissue in the Endoscope's Image**
>
> A tissue tracker finds the organ in the endoscope's images. In one research system a three-dimensional endoscope projects fringes onto the tissue to recover its surface, and a near-infrared camera follows biocompatible markers placed on it. The markers keep the track through blood and thin tissue, and the camera works 5 to 8 cm from the tissue, with the suturing tool withdrawn from the view so that it does not hide the surface [17]. A hidden landmark corrupts the measurement [18]. On a trend the report stops while the true organ moves on, as in case 8 at 60 s.

What Moves It

The instruments ride on an electromechanical arm under software control [20]. In the chapter the remote center is built into the joint coordinates. A research system of 2022 instead imposed the remote center as a constraint inside its kinematic solver, at the port of the laparoscopic tool [17]. The second-order servos of Equation (14.4), with their rate and acceleration limits, stand for the arm's joint drives.

> **TECHNOLOGY** **Final Element: The Cable-Driven Wristed Instrument**
>
> A dexterous surgical robot typically has seven degrees of freedom, including translations, rotations and the grip [13]. The wrist at the tip is driven by cables in sheaths, the most common drive of surgical tools for its small size, strength and flexibility. Friction between cable and sheath changes direction with the motor, so a tension reading shifts suddenly at a reversal before it settles, and a tension read near the motors carries that friction. A cable that sticks shows as an abnormal tension, and the robot can then stop itself [19]. The play and the give of Equation (14.5) stand for this drive in the model.

Where the Controller Runs

The surgeon's console and the patient-side arms are usually in the same operating room, where a survey puts the communication delay at 5 to 10 ms [18]. The controllers of this chapter act every 2 ms, and the model predictive option every 10 ms. The 2022 research system shows the same layers as the chapter: a task planner sends motion primitives to a trajectory generator, a kinematic solver turns them into joint trajectories, and closed-loop joint controllers follow them [17]. The console, the fixtures, the force loop and the compensation of Section 14.4 sit between the hand and that solver.

> **IN PRACTICE** **What the Regulator Asks of a Surgical Robot**
>
> In the United States, one rule for a software-controlled, table-mounted electromechanical system with instruments on an arm places it in Class II with special controls. The maker must run a training program for the device, distribute it only to facilities that maintain it, and report complaints and adverse events every year. Bench tests must show the device's motion accuracy and precision, instrument reliability and the human-device interface. Human factors validation must show safe use in an operating room, and the software needs verification, validation, hazard analysis and a review of its cybersecurity threats [20].

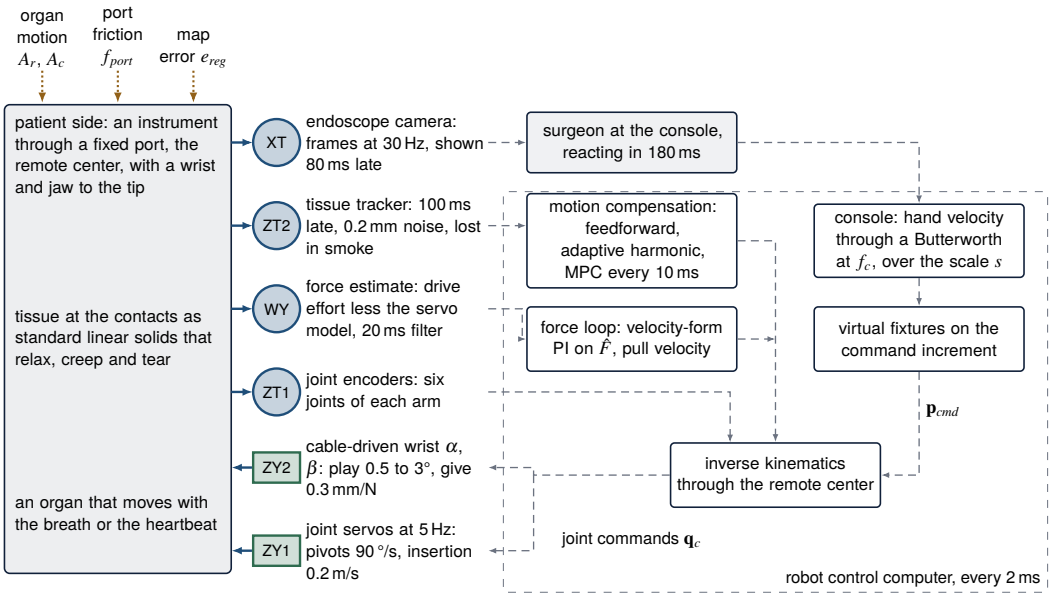


Figure 14.6 The loops of the chapter with real devices in place of the schematic's symbols. The surgeon sees the endoscope camera XT and moves the hand. A robot control computer acting every 2 ms scales and filters the hand in the console, bends the command at the virtual fixtures, adds the compensation learned from the tissue tracker ZT2, runs the force loop on the estimate WY, and solves the inverse kinematics for the joint servos ZY1 and the cable-driven wrist ZY2, read back by the encoders ZT1. Notice that the tip force has no sensor of its own, and that the surgeon closes the outer loop through a picture that is already late.

What Is Modernizing It

Autonomy is the first development. Research robots now plan and place sutures on soft tissue under supervision, and the operator approves or selects their plans [8, 17]. Sensing at the tip is the second. Fiber Bragg grating, capacitive and tactile sensors have been built for palpation, and a small tension sensor array at the distal end of a cable-driven robot is less affected by friction than one at the motors [19]. Motion compensation is the third. Telerobotic systems that synchronize the tool with an organ moved by breathing or the heartbeat have been studied for two decades, with position, force and impedance control schemes [18]. Security is the fourth. The United States rule for a mountable electromechanical surgical system asks for an assessment of the threats and vulnerabilities of its software as part of a cybersecurity review [20].

14.7 Limitations

The arms have exact kinematics and limited servos but no inertia, so a contact pushes the instrument back only through the wrist. Tissue is lumped at the contacts as standard linear solids with fixed tear limits, so a tear has no location, a needle cannot steer and the stretch of one bite does not load the next. The organ moves as a rigid body on a scripted shape, the ports are fixed, and there is no bleeding, smoke, port placement or haptic channel. The scripted surgeon is a forward-model controller with tremor and drift scaled by one pace, and it describes no person. Real surgeons adapt to a console, anticipate a breath and learn a worn instrument, and none of that is here. The error budget is measured at five seeds on three tasks and holds within those conditions, and the attribution on the moving kidney's bites was not resolved. Every tissue property, tolerance, ceiling, latency and time budget was chosen for teaching and carries no clinical meaning. Without a learning study, nothing is claimed

about what students learn, and the simulator is not a surgical trainer, clinical software or a decision aid.

OPEN CHALLENGE **Feeling the Tissue Through the Robot**

The lack of effective haptic feedback is often reported as a major limitation of teleoperated surgical robots. A perfectly transparent teleoperator would need perfect models of both robots, zero delays and perfect force sensing or estimation, and pushing toward transparency lets small errors and delays cause oscillations that surgery cannot accept. Force sensors at the tip must also meet limits on size, cost, biocompatibility and sterilization [13]. Progress would be an affordable, sterilizable instrument that senses its tip force, displayed to the hand without loss of stability.

14.8 Conclusion

A surgical robot realizes the hand's intent through a point that must not move, and this simulator measures what each layer of that realization costs. The inversion of the fulcrum is exact until the tip nears the port, where the pivots reach 90 °/s and the tip falls 51.5 mm behind. A 6 Hz filter at 3:1 keeps the hand off the artery that a 2 Hz filter overshoots into by 0.95 mm. A held position slips at 11.5 s, and a force loop at 2.5 N tears its flap by creep at 13.3 s. On the breathing kidney the adaptive predictor holds the tip at 1.10 mm RMS against 3.29 mm by hand, and on the heart no setting does better than 1.53 mm. The factorial budget places 86 % of the hold's mean-square error in the interaction of the surgeon's delay with the organ's motion and shows the predictor removing 91 % of it. The model is lumped, rigid and scripted. A fuller model would add arm dynamics, a deforming organ and a haptic channel with its stability limits, and only a study of students using the cases could say what they learn. The simulator is a surgical robot that can be taken apart one control layer at a time.

KEY POINTS

- A surgical robot carries out the hand's intent through a point that must not move.
- Inverting the fulcrum is exact until the tip nears the port, where the pivots saturate.
- At 3:1 a 6 Hz filter keeps the hand off the artery, and a 2 Hz filter overshoots into it.
- A position hold fails slowly by relaxation, and a force hold by creep.
- The surgeon's delay interacting with the organ's motion holds 86 % of the hold's mean-square error, and the predictor removes 91 % of it.

Where else this applies. A disturbance on a measured period also drives the tooth-passing vibration of Volume 7, Chapter 13.

References

[1] S. Hara, Y. Yamamoto, T. Omata, and M. Nakano, "Repetitive control system: A new type servo system for periodic exogenous signals," *IEEE Transactions on Automatic Control*, vol. 33, no. 7, pp. 659–668, 1988.

[2] R. Ginhoux, J. Gangloff, M. de Mathelin, L. Soler, M. M. A. Sanchez, and J. Marescaux, "Active filtering of physiological motion in robotized surgery using predictive control," *IEEE Transactions on Robotics*, vol. 21, no. 1, pp. 67–79, 2005.

[3] O. Bebek and M. C. Cavusoglu, "Intelligent control algorithms for robotic-assisted beating heart surgery," *IEEE Transactions on Robotics*, vol. 23, no. 3, pp. 468–480, 2007.

[4] R. H. Taylor, J. Funda, B. Eldridge, S. Gomory, K. Gruben, D. LaRose, M. Talamini, L. Kavoussi, and J. Anderson, "A telerobotic assistant for laparoscopic surgery," *IEEE Engineering in Medicine and Biology Magazine*, vol. 14, no. 3, pp. 279–288, 1995.

[5] R. H. Taylor and D. Stoianovici, "Medical robotics in computer-integrated surgery," *IEEE Transactions on Robotics and Automation*, vol. 19, no. 5, pp. 765–781, 2003.

[6] C. N. Riviere, R. S. Rader, and N. V. Thakor, "Adaptive cancelling of physiological tremor for improved precision in microsurgery," *IEEE Transactions on Biomedical Engineering*, vol. 45, no. 7, pp. 839–846, 1998.

[7] S. A. Bowyer, B. L. Davies, and F. Rodriguez y Baena, "Active constraints/virtual fixtures: A survey," *IEEE Transactions on Robotics*, vol. 30, no. 1, pp. 138–157, 2014.

[8] A. Shademan, R. S. Decker, J. D. Opfermann, S. Leonard, A. Krieger, and P. C. W. Kim, "Supervised autonomous robotic soft tissue surgery," *Science Translational Medicine*, vol. 8, no. 337, 2016.

[9] Y.-C. Fung, *Biomechanics*. New York, NY: Springer, 1993.

[10] A. M. Okamura, C. Simone, and M. D. O'Leary, "Force modeling for needle insertion into soft tissue," *IEEE Transactions on Biomedical Engineering*, vol. 51, no. 10, pp. 1707–1716, 2004.

[11] Y. S. Kwoh, J. Hou, E. A. Jonckheere, and S. Hayati, "A robot with improved absolute positioning accuracy for CT guided stereotactic brain surgery," *IEEE Transactions on Biomedical Engineering*, vol. 35, no. 2, pp. 153–160, 1988.

[12] A. G. Gallagher, N. McClure, J. McGuigan, K. Ritchie, and N. P. Sheehy, "An ergonomic analysis of the fulcrum effect in the acquisition of endoscopic skills," *Endoscopy*, vol. 30, no. 7, pp. 617–620, 1998.

[13] A. M. Okamura, "Haptic feedback in robot-assisted minimally invasive surgery," *Current Opinion in Urology*, vol. 19, no. 1, pp. 102–107, 2009.

[14] J. Marescaux, J. Leroy, M. Gagner, F. Rubino, D. Mutter, M. Vix, S. E. Butner, and M. K. Smith, "Transatlantic robot-assisted telesurgery," *Nature*, vol. 413, no. 6854, pp. 379–380, 2001.

[15] K. H. Sheetz, J. Claflin, and J. B. Dimick, "Trends in the adoption of robotic surgery for common surgical procedures," *JAMA Network Open*, vol. 3, no. 1, p. e1918911, 2020.

[16] R. H. Thompson, B. R. Lane, C. M. Lohse, B. C. Leibovich, A. Fergany, I. Frank, I. S. Gill, M. L. Blute, and S. C. Campbell, "Every minute counts when the renal hilum is clamped during partial nephrectomy," *European Urology*, vol. 58, no. 3, pp. 340–345, 2010.

[17] H. Saeidi, J. D. Opfermann, M. Kam, S. Wei, S. Leonard, M. H. Hsieh, J. U. Kang, and A. Krieger, "Autonomous robotic laparoscopic surgery for intestinal anastomosis," *Science Robotics*, vol. 7, no. 62, p. eabj2908, 2022.

[18] L. Cheng and M. Tavakoli, "COVID-19 pandemic spurs medical telerobotic systems: A survey of applications requiring physiological organ motion compensation," *Frontiers in Robotics and AI*, vol. 7, p. 594673, 2020.

[19] Z. Zhou, J. Yang, M. Runciman, J. Avery, Z. Sun, and G. Mylonas, "A tension sensor array for cable-driven surgical robots," *Sensors*, vol. 24, no. 10, p. 3156, 2024.

[20] U.S. Food and Drug Administration, "Mountable electromechanical surgical system for transluminal approaches," Code of Federal Regulations, Title 21, Section 878.4961, revised as of April 1, 2024, U.S. Government Publishing Office, govinfo.gov, 2024.

14.9 Exercises

14.1 ⌕ Concept check · 2 min

In case 3 at a motion scale of 3:1, lowering the tremor filter cutoff from 6 to 2 Hz cuts the tremor at the tip from 31 to 12 µm, yet three strokes now reach the cystic artery where none did at 6 Hz. What causes the contacts?

(a) The 2 Hz filter passes more of the 10 Hz tremor than the 6 Hz filter does

(b) The shaft's pivots reach their 90 °/s limit near the port during each stroke

(c) At a low cutoff the console no longer divides the hand's drift by the motion scale

(d) The filter's lag is missing from the surgeon's forward model, so the surgeon pushes on past the target

14.2 ⌕ Concept check · 1 min

In case 4 a force loop holds the bladder flap at 2.5 N, below the flap's 3 N tear force, and the flap tears at 13.3 s. Why?

(a) Under a held force the flap creeps, and its stretch passes the 10 mm stretch limit

(b) Port friction biases the estimate low, so the true force climbs past 3 N

(c) The integral term winds up, and the arm overshoots the setpoint past the tear force

(d) The force relaxes below the 0.7 N the dissection needs, and the slipping flap tears

14.3 Concept check · 2 min

In case 5 the virtual fixture is on, but its region is registered 4 mm off, toward the path of the dissection. What does the run show?

(a) The tip enters the true region twice, because the shifted map admits the path

(b) Nothing enters the true region, but the fixture holds the tip in safe tissue for several seconds

(c) The tip chatters at the edge of the region, because the fixture pushes it out at $50\,\mathrm{s}^{-1}$

(d) Nothing changes, because the fixture is judged against the true region and not the map

14.4 Theory and calculation · 5 min

In case 1 a straight instrument of 360 mm is held by its handle with 120 mm inside the port. In case 2 the robot holds the same kind of shaft, whose pitch and yaw are limited to 90 °/s.

(a) Use Equation (14.3) to find the tip motion for a 20 mm move of the hand, before and after the instrument is pushed in by 80 mm. *Checkpoint:* −10.0 mm and −25.0 mm.

(b) Find the sideways tip speed the pivot limit allows at an insertion of 105 mm and of 30 mm. *Checkpoint:* 165 mm/s and 47.1 mm/s.

(c) At one to one the hand moves at up to 0.15 m/s. Find the pivot rate that speed needs at 30 mm of insertion, as a multiple of the limit. *Checkpoint:* 5.0 rad/s, or 286 °/s, 3.2 times the limit.

14.5 Theory and calculation · 8 min

The console filters the hand's velocity with a second-order Butterworth low-pass of cutoff f_c. Its gain at a frequency f is $1/\sqrt{1+(f/f_c)^4}$, and its phase lag is $\varphi = \arctan\bigl(\sqrt{2}\,r/(1-r^2)\bigr)$ with $r = f/f_c < 1$, a delay of $\varphi/(2\pi f)$.

(a) Find the share of a 10 Hz tremor that passes at $f_c = 6$ and at 2 Hz, and the tremor left in the command at a scale of 3:1 if the hand's 0.3 mm RMS were all at 10 Hz. *Checkpoint:* 0.339 and 0.040, so 34 µm and 4.0 µm.

(b) Find the delay each filter adds to a 1 Hz motion. *Checkpoint:* 37.9 ms and 120.3 ms.

(c) The surgeon's loop is an integrator of gain $K = 2\pi\ \mathrm{s}^{-1}$. Use Equation (1.16), whose loop gain Kk_i is here the surgeon's K, to find its delay margin, and compare it with the 0.26 s the surgeon's image is late. *Checkpoint:* 0.25 s, less than 0.26 s.

(d) The forward model covers the 0.26 s and nothing else. How much more unmodeled delay does the 2 Hz filter add at 1 Hz than the 6 Hz filter? *Checkpoint:* 82.4 ms.

14.6 Theory and calculation · 8 min

The bladder flap of case 4 is a standard linear solid, Equation (14.6), with $k_e = 150\,\mathrm{N/m}$, $k_m = 250\,\mathrm{N/m}$, $\tau = 4\,\mathrm{s}$ and $x_0 = 15\,\mathrm{mm}$. It tears at 3 N or at 10 mm of stretch, and the dissection needs 0.7 N.

(a) The arm holds a stretch of 4 mm. Find the force at once, with $x_m = 0$, and the force once fully relaxed. Does the hold keep 0.7 N? *Checkpoint:* 1.64 N and 0.64 N, so no.

(b) Find the share of the linear force a held stretch loses and the time constant of creep under a held force. *Checkpoint:* 0.625 and 10.7 s.

(c) A force loop holds the true force at its setpoint once the arm is at rest. Find the relaxed stretch at 0.8 N and at 2.5 N. *Checkpoint:* 4.83 mm and 10.90 mm.

(d) Find the smallest setpoint at which the flap tears by creep, however long it takes. *Checkpoint:* 2.17 N.

14.7 App challenge · 8 min

Load scenario 4, Hysterectomy: holding the flap. It ships with the Force loop in Position (MAN) at a pull depth of 4.00 mm. Use the default seed, run each case for 120 s at a playback speed of 5, and export the CSV file after each run.

(a) Run as shipped. Read the Peak tissue force tile and the true force on the Flap force tile at 120 s, and find the first row in which column `slip` reads 1. *Checkpoint:* 1.64 N, 0.64 N and 11.5 s, within 0.05 s.

(b) Press Reset, set the Force loop to Force (AUTO) with the Force setpoint at 0.80 N, and run again. Read column `flap_stretch_m` at 10 and at 120 s. *Checkpoint:* 3.61 mm and 4.83 mm, within 0.02 mm.

(c) Press Reset, set the Force setpoint to 2.50 N, and run again. Find the first row in which column `tears` reads 1. *Checkpoint:* 13.3 s, within 0.1 s.

Compare (b) and (c) with the relaxed stretches of the flap calculation earlier in this set.

14.8 App challenge · 6 min

Load scenario 7, Colectomy: the stapler. The jaws close on the colon at 10 s, and the stapler fires after the Wait before firing, 0 s as shipped. Use the default seed and a playback speed of 5, and run each case until the stapler has fired and the run pauses.

(a) Run as shipped. Then press Reset, set the wait to 15 s and run. Then press Reset, set it to 45 s and run. Read the Staple-line stress tile each time. *Checkpoint:* index 2.24 at 1.57 N, 1.46 at 1.02 N, 1.06 at 0.75 N.

(b) The index is the force at firing over the fully relaxed force at the same gap. From the first run alone, find the relaxed force. Then predict the index after 15 and 45 s if its excess over one decays with the bowel's relaxation time of 15 s. *Checkpoint:* 0.70 N, then 1.46 and 1.06.

14.9 App challenge · 8 min

Load scenario 8, Partial nephrectomy: the breathing kidney. Use the default seed and a playback speed of 5, and run each case for the full 90 s. Run first with Motion compensation None, as shipped, then press Reset and run with Ventilator feedforward, then Adaptive harmonic, then MPC.

(a) Read the Tracking error tile, the RMS distance from the mark from 10 s, for each option. *Checkpoint:* 3.29, 2.19, 1.10 and 1.13 mm, within 0.01 mm.

(b) Read the During the dropout tile for None and for Adaptive harmonic. *Checkpoint:* 4.51 mm and 4.49 mm, within 0.02 mm.

Explain why feedforward falls short of the predictor, why MPC is no better than the predictor, and why the dropout costs every option the same.

14.10 Application area · 4 min

The tip force is not measured. It is estimated from the drive's effort, which carries the port's Coulomb friction of 0.3 N along the shaft, Equation (14.9). In case 10 each suture is pulled until the estimate reads 0.5 N, and the scorecard reports a true tension of 0.28 N.

(a) By how much, in newtons and as a share of the truth, does the estimate read high, and which way was the shaft sliding? *Checkpoint:* 0.22 N, 79 % of the truth, sliding outward.

(b) Name two changes a design engineer could make so that the pull reaches its intended tension.

14.11 Application area · 4 min

Case 11 asks the tip to stay within 1 mm of a coronary artery on a heart beating at 72 beats per minute, each beat drawn within ±5 % of the mean, behind 5 Hz joint servos.

(a) Find the period of the motion and the frequency of its third harmonic, and repeat the harmonic at 100 beats per minute. *Checkpoint:* 0.83 s and 3.6 Hz, then 5.0 Hz.

(b) A beat 5 % longer than the last is read on the phase of the last interval. Find the largest phase error. *Checkpoint:* 18°.

(c) Name the surgical answer to this motion and say why it is not a control setting.

14.12 Review the agent · 5 min

A student asks an AI assistant how to improve the hold on the breathing kidney of case 8. The assistant replies: “Table 14.6 shows that the delay-times-motion term is 86 % of the mean-square error without compensation. The tracker reports 100 ms late, so set the Tracker latency to 40 ms. That removes most of the delay and with it most of the error.” Find the flaw and say how to check it in the app.